



## Research article

Formulation of alginate based hydrogel from brown seaweed, *Turbinaria conoides* for biomedical applications

Naidu Kavitha<sup>a</sup>, Thennarasu Padmini Karunya<sup>b</sup>, Shankar Kanchana<sup>a</sup>, Kumar Mohan<sup>a</sup>,  
Ramachandiran Sivaramakrishnan<sup>a</sup>, Selvaraj Uthra<sup>a</sup>, Kalimuthu Kapilan<sup>a</sup>,  
Dinakarkumar Yuvaraj<sup>b</sup>, Muthuvel Arumugam<sup>a,\*</sup>

<sup>a</sup> CAS in Marine Biology, Faculty of Marine Sciences, Annamalai University, Parangipettai, Tamil Nadu, India, 608502

<sup>b</sup> Department of Biotechnology, Vel Tech High Tech Dr. Rangarajan Dr. Sakunthala Engineering College, Chennai, Tamil Nadu, India, 600062

## ARTICLE INFO

## Keywords:

Materials science  
Materials chemistry  
Biomedical engineering  
Pharmaceutical science  
Biotechnology  
Hydrogel  
Microfilm  
Microbead  
Wound healing  
Drug delivery  
Sustained release

## ABSTRACT

Sodium Alginate (SA) is an excellent carrier in various drug delivery systems. In this study, SA was synthesized from brown seaweed, *Turbinaria conoides* with a yield of  $31.3 \pm 0.86\%$ . The analysis of physicochemical properties of extracted alginate (ALG) determined its purity. The structural confirmations of ALG were studied through FTIR, XRD and SEM analysis. Formulation of ALG with collagen (COL) as a wound healing microfilm showed potential anti-inflammatory properties ( $81.3 \pm 1.77\%$ ) and sustained drug release. Likewise, the ALG microbead encapsulated with an anticancer drug, Tamoxifen indicated an *in vitro* sustained release in the range of  $62 \pm 0.70\%$  -  $91 \pm 0.56\%$ . The overall swelling behavior of both the hydrogels, microfilm and microbead provides new opportunities for development of natural ALG in this therapeutic era.

## 1. Introduction

The marine environment has evolved over millions of years and is a rich source of genetic diversity and novel pharmaceutical ingredients. With only 16% of marine life been identified so far, the rate of discovery of marine species has been higher than terrestrial species since the 1950s [1]. The marine environment broadly consists of marine flora and fauna [2]. The flora includes seaweed, seagrass and mangroves that are a taxonomically diverse and chemically rich group of marine organisms.

Seaweeds are macroscopic flora that originates on the rocky bottom in relatively shallow coastal water. These are prospective renewable resources in the marine realm with about 6000 species identified so far. They are categorized into three different classes such as Green Seaweed (Chlorophyceae), Brown Seaweed (Phaeophyceae) and Red Seaweed (Rhodophyceae). According to Food and Agriculture Organization (FAO) [2016], the global production of seaweed has crossed 30 million tons of fresh weight year<sup>-1</sup> with an average value of \$400 tons per dry weight [3].

The polysaccharide ALG is found in the cell walls of Phaeophyceae, provides it with flexibility [4]. SA is a natural derivative of this polysaccharide and is soluble in both cold and hot water when subjected to strong agitation. Factors such as pH, concentration, ions in solution and the presence of divalent ions are responsible for the solubility of SA [5]. It also has a property to thicken as well as bind. In the presence of calcium, SA forms a gel without the need for heat.

In modernist cuisine, SA is mostly used with calcium salts to produce small and large spheres with liquid inside that burst in the mouth and as a thickener in the food industries [6]. ALG has numerous applications in biomedicine due to its ideal characteristics such as biocompatibility and ease in gelation. These are attractive hydrogels for wound healing, drug carrier and tissue engineering applications. Such hydrogels have relative similarity to the extracellular matrices of living tissues and can be modified for several valuable biomedical applications [7].

ALG hydrogel comprises hydrophilic structures that withstand huge content of water in their three-dimensional linkages. Considerable use of these products in different industries and environments demonstrates their importance [8]. Among the various biologics combined with ALG in

\* Corresponding author.

E-mail address: [arucasm@gmail.com](mailto:arucasm@gmail.com) (M. Arumugam).

biomaterial science, COL has been extensively used for wound healing and tissue regeneration [9, 10]. However, very few marine-based COL are combined with ALG of similar origin. Likewise, the applications of ALG as drug carriers of anticancer drugs, Tamoxifen are still being interrogated as a prevalent area of research [11].

ALG based hydrogels have multipotent applications in the field of biomedical sciences. It is usually synthesized in the form of  $\text{Na}^+$ ,  $\text{Ca}^{2+}$ ,  $\text{Ba}^{2+}$ ,  $\text{Mg}^{2+}$ ,  $\text{Fe}^{2+}$  and  $\text{Al}^{3+}$  [12]. Previously, a multilayered ALG/Chitosan complex was used for the delivery of the anticancer drug, tamoxifen [11]. In addition, the efficiency of COL and ALG based hydrogels has been for the prevention of rat chondrocyte dedifferentiation [13]. Bio-inspired collagen/alginate/fibrin-based hydrogels were synthesized for the regeneration of pancreatic tissue engineering and musculoskeletal applications [14]. However, commercial SA has been utilized in these biomedical applications. To the best of our knowledge, there are lacunae in the available literature that has explored the combination of ALG with stingray fish collagen for wound healing application.

Thus, in the present investigation, ALG was extracted, purified and combined with stingray fish COL as microfilm with wound healing properties whereas, Tamoxifen encapsulated within ALG microbeads was formulated as a drug delivery system.

## 2. Materials and methods

### 2.1. Chemicals & reagents

Diclofenac sodium and Tamoxifen was obtained as a gift sample from Mugunthan Pharmacy, Parangipettai. Calcium Chloride, Sodium Carbonate and Bovine Serum Albumin (BSA) were purchased from HiMedia Laboratories, Mumbai. Glycerol anhydrous GR (GLY) was obtained from Merck, India. All other analytical grade solvents and chemicals used in the present study were procured from Fisher Scientific, India.

### 2.2. Sample collection

The brown seaweed, *T. conoides* was hand-picked at a depth of 2 ft from the coastlines of Mandapam (Latitude  $9^{\circ}28'N$  and Longitude  $79^{\circ}15'E$ ), Tamil Nadu. The samples were washed with seawater to eliminate the debris or epiphytes and sun-dried for 2 d. The parched materials were brought to the laboratory and were rinsed thoroughly under tap water to remove the traces of salt and sand particle. The seaweed was dried under shade for 7 d and minced using a fine scalpel. The seaweed powder was sieved to achieve a particle size of 0.5–1.0 mm and stored in sealed plastic bags under the dark condition for further analysis.

### 2.3. Extraction of SA

The extraction of SA was performed by following Fenoradosa [15] with minor modifications. About 40g of seaweed powder was weighed and soaked in 1200 ml of 1.5% formaldehyde for 24 h at room temperature under dark conditions. Later, this content was rinsed with distilled water (DW) and 1200 ml of 0.2M HCl was added for incubation under the same condition for another 24 h. The sample was again rinsed with DW to remove the acid traces. Further, thrice the volume of sodium carbonate was added and the mixture was heated for 5 h at  $60^{\circ}\text{C}$ . This content was then centrifuged at 3000 rpm for 20 min and its supernatant was collected. For precipitating of SA, thrice the volume of 99.9% ethanol was added to the extract. The precipitate was centrifuged at 1000 rpm for 10 min and was purified by acetone treatment. In this, 50 ml acetone was added to the ALG and the whole was again centrifuged at 1000 rpm for 10 min at the duplicate time. The collected precipitate was dried at  $60^{\circ}\text{C}$  to remove the acetone content; dissolved in DW for rinsing and concentrated at  $60^{\circ}\text{C}$  for 5 h. Further, thrice the volume of this concentrated mixture, 95% ethanol was added for re-precipitation of SA. The precipitated ALG was collected after centrifugation at 1000 rpm for

10 min, dried at  $60^{\circ}\text{C}$ , dialyzed against DW and lyophilized to obtain pure ALG powder.

### 2.4. Evaluation of physical parameters

The solubility of SA in various solvent systems was examined. In this test, 100 mg of dried extract was mixed with 1 ml of DW, ethyl alcohol, methanol, dimethylsulfoxide (DMSO), acetone, chloroform, dichloromethane (DCM), n-hexane, n-butanol, HCl and  $\text{H}_2\text{SO}_4$ . For the dissolution of the sample in organic solvents, mild agitation was provided by mechanical stirring. The pH of SA was measured using a pH meter (Eco Testr pH1, Thermo Scientific) by dissolving 1g of it in 100 ml of distilled water. Around 100 mg of SA was weighed and transferred to a pre-weighed and dry Petri dish for quantification of the moisture content. Then, the SA was subjected to heating at  $105 \pm 1^{\circ}\text{C}$  for 1 h. Further, the Petri plate was cooled in a desiccator and the attained constant weight was noted after the successive repetition of the experiment. The formula used for this study is as expressed in (1).

$$\text{Weight of moisture and volatile substances} = (W_1 \times 100)/W \quad (1)$$

Where

$W_1$  = Loss in material (g) after dryness.

W = Weight of SA (g) before heating.

### 2.5. Compositional and FT-IR analysis of SA

The compositional analysis of purified SA was performed in triplicate. The protein content was analyzed by Lowry's method [16]. Carbohydrate was estimated by Dubois et al. [17] and uronic acid content was evaluated following the method of Bitter and Muir [18]. The phytochemical components were qualitatively analyzed by using different standardized test procedures [19]. The FT-IR analysis of SA powder extracted from seaweed was carried out to analyze the functional groups by the KBr pellet method.

### 2.6. XRD analysis

The X-ray diffractometer (XRD) facility at the Department of Nuclear Physics, University of Madras (Guindy) was used for determining the phase existence of extracted SA. The ambient conditions for analysis were set as  $\text{Cu K}\alpha$  ( $\lambda = 1.5406 \text{ \AA}$ ) as a radiation source at the current 15 mA with voltage 40kV. The spectra of XRD are recorded at  $2\theta = 10.0227^{\circ}$  to  $89.9597^{\circ}$  at a scanning speed  $1^{\circ}/\text{min}$  and step size at  $0.0430^{\circ}$ . The obtained XRD peaks were compared with standard reference Joint Committee of Powder Diffraction Standards (JCPDS) file for SA.

### 2.7. Formulation of ALG microfilm with wounding healing properties

#### 2.7.1. Preparation of ALG based microfilm

The hydrogel films were prepared as per the methodology of Pereira [20] with minor modifications. Purified SA from *T. conoides* and COL from stingray fish skin were used in the formulation. Further, the hydrogels were formulated by the 'solvent-casting' technique. The SA dissolution (1.5% w/v) in DW and 0.5% COL in 3% acetic acid solution were carried under magnetic stirring at 600 and 400 rpm respectively. The plasticizer agent, GLY was added at 15% (w/w) of SA. Then, this solution was degassed for 12 h at room temperature. An experiment was performed for identifying the ideal mold for the casting of the hydrogels. In this process, aluminum foil as cube molds and Petri dishes (5 and 12 cm in diameter) were used in this study. The casting and recovery of microfilm were feasible from the 12 cm Petri dish. Around, 18 ml of SA mixture was found to be ideal for the casting of the microfilms in the selected mold with and without the incorporation of GLY. The resultant

microfilms were designated as SAG and SA respectively. The SA and COL were added in the ratio of 60:40 and 90:10 with and without glycerol.

### 2.7.2. Film transparency and transmission assay

The hydrogel transparency and light transmission spectrophotometrically determined according to Norajit [21]. Samples were cut into rectangular films, placed inside a cuvette and their light blockade features were recorded at a wavelength between 200 and 800 nm while using air as control. The film transparency was calculated using the following formula (2).

$$\text{Transparency} = \text{Abs}_{600} / x \quad (2)$$

Where x is the thickness of the film measured in  $\mu\text{m}$ .

### 2.7.3. Measurement of swelling behavior

A small rectangular film was cut in the dimension of  $1 \times 1$  cm and weighed. The film was then placed in 20 ml phosphate buffer saline (pH 7.4) in a Petri plate. The hydrogel was taken out of buffer after 30 min and reweighed. Thus, the swelling behavior was measured as a '% swelling index' (3)

$$\% \text{swelling index} = [(W_h - W_d) \times 100] / W_d \quad (3)$$

$W_h$  is the weight of the product after 30 min of hydration and  $W_d$  is the weight of the dried product.

### 2.7.4. Protein denaturation assay

The reaction mixture comprised of 0.45 ml of bovine serum albumin (5% aqueous solution) and 0.05 ml purified SA (50  $\mu\text{g}/\text{ml}$ ). The pH of this mixture was maintained at 7.4 with a few drops of 1 N Hydrochloric acid. The samples were maintained at 37 °C for 20 min and then warmed for 3 min at 57 °C. The tubes were cooled and 2.5 ml of phosphate buffer solution was further mixed. Turbidity was recorded at 660 nm for control which consists of 0.05 ml DW only. The inhibition of protein denaturation (%) was calculated as per the formula of Gunathilake [22] and expressed in (4).

$$\% \text{ inhibition of denaturation} = 100 \times (1 - A_2/A_1) \quad (4)$$

where  $A_1$  = absorption of the standard and  $A_2$  = absorption of the SA.

## 2.8. Preparation and encapsulation of anticancer drug in ALG microbead

The SA beads were prepared according to the method described by Mandal [23]. The beads were prepared by extruding 1% and 2% SA aqueous solution and Tamoxifen (5% and 10%) through a micropipette into 10 mM  $\text{CaCl}_2$  aqueous solution and cured for 1 h. The resultant SA gel beads were washed with DW. The swelling behavior of the bead was calculated as described in section, 2.7.3.

### 2.8.1. Drug entrapment efficiency (DEE)

30 mg of drug-containing ALG beads were suspended into 30 ml of phosphate buffer saline whose pH was maintained at 7.4 and was left for 24 h at room temperature. After the incubation period, the beads were stirred at 50 rpm on a magnetic stirrer for 15 min. The mixture was filtered after stirring and 5 ml of the solution was taken which was then diluted to 100 ml by adding 95 ml of phosphate buffer saline. The absorbance was recorded at 276 nm in a spectrophotometer.

### 2.8.2. In vitro drug release studies

In this study, 30 mg of beads containing the drug were accurately weighed and was added to 270 ml of 0.1N HCl for 2 h. After the incubation period, the test was continued by transferring the beads into 30ml phosphate buffer saline (pH 7.4) for the next 10 h, stirred gently at a magnetic stirrer. The sample was withdrawn at an equal interval of 1 h, filtered and the absorbance was measured at 276 nm in a spectrophotometer. The equal volume of fresh solution was added every time the sample was withdrawn.

## 2.9. Statistical analysis

Statistical analysis was performed using the SPSS Version 11.0 software. The data were expressed as mean  $\pm$  standard deviation (SD). All the experiments were performed in triplicates.

## 3. Results and discussion

The aim of this study was to extract SA from *T. conoides* and determine its suitability for use in a hydrogel, microfilm for wound healing applications and as a microbead for delivery of an anticancer drug.

The yield of the extracted SA was found to be  $31.3 \pm 0.86\%$ . Seasonal and temporal changes greatly influence the yield of ALG from a particular species. The obtained yield was found to be higher than the yield reported by Kusumawati [24] for *T. conoides* ALG isolated from Binuangen beach, Banten, Indonesia. Further, the yield of ALG of *T. conoides* collected during 1998–99 ranged from 26.0% to 38.0% in the leaf; 22.0%–29.0% in stem and 11.0%–24.0% in thallus [25].

### 3.1. Physical properties

The pH of 1% SA of *T. conoides* solution was  $8.1 \pm 0.8$ . In this context, McDowell [26] stated in his study that the addition of acid or base which brings the pH of ALG solution below 5 or above 9 will accelerate depolymerization of the ALG. Hence, as the obtained pH was between the polymerization ranges, the purity of the ALG could be partially affirmed. Subsequently, the moisture content recorded for the alginic acid was  $10 \pm 0.2\%$ . Kusumawati [24] has also reported the moisture content of *Turbinaria* sp. in their work as 14.77 %, which is higher than the content reported in the present study. It is to be noted that lower the moisture content, better is the shelf life of the sample. Nasir [27] reported that the high moisture content could result in the faster growth of fungi and insect's infestation. Hence lower the moisture content of SA powder, the longer is its shelf life. The extracted SA was easily soluble in HCl,  $\text{H}_2\text{SO}_4$  and DW. It was not soluble in ethyl alcohol, methanol, DMSO, acetone, chloroform, DCM, n-hexane and n-butanol. As the sodium salt of alginic acid is a water-soluble polymer, it was readily soluble in DW [28].

### 3.2. Biochemical composition

The physicochemical parameters of SA were determined by calculating Carbohydrate content ( $48.46 \pm 1.57\%$ ), Protein (0%) and Uronic acid ( $9.0 \pm 0.31\%$ ). Kokilam [29] reported a higher carbohydrate level ( $59.30 \pm 0.66\%$ ) in *Padina tetrastromatica* and protein concentration ( $15.34 \pm 0.01\%$ ) in *Hormophysa triquetra*. This difference in carbohydrate could be due to the association of polyphenolic and other constituents with the alginic acid that is innately present in the seaweed. However, in the case of protein content, the lesser the value indicates higher the purity of the extracted ALG. Moreover, Larsen [30] estimated the glucuronic and mannuronic content in the ALG extracted from brown seaweed, *S. asperifolium* from the Egyptian coast as 78 mg and 80 mg respectively. As a direct comparison could not be done in this case, it may be understood that uronic acid composition plays a significant role in the structure of ALG. Larsen [31] indicated that uronic acid residues exist as homopolymers of either D-mannuronic acid residues (M-blocks) or L-glucuronic acid residues (G-blocks), distanced by MG-blocks, arranged in a nearly alternating fashion.

The phytochemical analysis revealed the absence of alkaloids, tannins, phlobatannins, flavonoids, steroids, terpenoids, glycosides and phenols. Only saponins (sugar derivatives) were found to be present in the SA, which confirmed the better purity of the extracted ALG. Kumar [32] stated the absence of alkaloids, steroids, flavonoids, saponins, tannins and phenols, however, the chemical component carbohydrate was only present that confirmed the purity of this polysaccharide. The

presence of saponins a type of glycosides is commonly found as secondary metabolites in both marine as well as terrestrial beings. It consists of one steroid and carbohydrate moiety in its structure [33]. Thus, as only the derivative of carbohydrates, saponin was present, the chemical purity of the SA could be completely affirmed.

The FT-IR analysis of SA powder (Figure 1) showed a characteristic peak at  $3460.90\text{ cm}^{-1}$  because of the intermolecular hydrogen-bonded -OH group. Notably, weak bands at  $2927$  and  $2107\text{ cm}^{-1}$  was due to -CH stretching and -OH bending peaks at  $1034.94$ ,  $1089.66$  and at  $1260.46\text{ cm}^{-1}$ , may be assigned to C-C-H and O-C-H deformation, C-O stretching and C-O and C-C stretching vibrations of pyranose rings. The anomeric, region ( $950\text{--}750\text{ cm}^{-1}$ ) signified an important region in the carbohydrates. The band at  $952.07\text{ cm}^{-1}$ , was assigned to the C-O stretching vibration of uronic acid and one at  $902.83\text{ cm}^{-1}$  assigned to the C-H deformation vibration of  $\beta$ -mannuronic acid residues. The bands at  $895.56\text{ cm}^{-1}$ ,  $848.86\text{ cm}^{-1}$  and  $819.89\text{ cm}^{-1}$  seem to be characteristic of mannuronic acid residues. Li [34] cited the -OH groups of ALG were observed at  $3400\text{ cm}^{-1}$ . They highlighted that peaks for -CH<sub>2</sub> groups in ALG were represented at  $2931\text{ cm}^{-1}$  and  $2926\text{ cm}^{-1}$  and distinctive peaks of the carboxyl group with strong absorption bands at  $1614\text{ cm}^{-1}$ ,  $1416\text{ cm}^{-1}$  and  $1306\text{ cm}^{-1}$  respectively. The band at  $1648\text{ cm}^{-1}$  was attributed to the carbonyl stretching (-HC = O). Similar FT-IR spectra for ALG extracted from *T. turbinata*, *S. filipendula*, *Dictyota caribaea* and *Padina perindusiata* collected at Yucatan Peninsula (Mexico) has been reported by García-Ríos [35].

### 3.3. XRD spectra

The XRD spectral analysis confirmed the presence of SA. There were two major diffraction peaks at  $2\theta$  values,  $13.764^\circ$  and  $22.020^\circ$  (Figure 2). These are characteristic peaks of the pure crystalline form of SA. SA is usually crystalline due to strong interaction between the ALG chains through intermolecular hydrogen bonding [36]. The obtained XRD spectra were in correlation with the findings of Helmiyati and Aprilliza [37]. The isolated ALG from brown seaweed collected in Indonesia and observed diffraction peaks at angles,  $22.90^\circ$ . Further, diffraction peaks at  $2\theta$  values  $13.5^\circ$ ,  $22^\circ$  and  $39^\circ$  were observed for SA (commercial) which is similar to the results obtained in the present study [38].

### 3.4. ALG film preparation

In the present work, hydrogel films composed of ALG and COL from brown seaweed and stingray fish respectively were developed for application in both exuding and dry wounds. Key properties such as thickness, transparency, swelling behavior and *in vitro* degradation were tested to evaluate the potential of these films as wound dressing agents. The films were cast on different molds made up of aluminum foil and Petri dish of two different dimensions such as 5 cm and 12 cm diameter at a thickness of half an inch (Figure 3). The recovery from the 12 cm diameter Petri dish was more efficient when compared to the other tested molds. Hence, the 12 cm Petri plate mold was selected for gel casting.

#### 3.4.1. Film thickness

The developed ALG/COL films consisted of a smooth surface, high malleability and thicknesses comprised around  $50.1 \pm 1.8\ \mu\text{m}$  to  $64.6 \pm 1.5\ \mu\text{m}$  (Table 1). The incorporation of COL within the ALG film caused a significant increase in the film thickness when compared with the SA film. While the thickness of the ALG/COL GLY films was significantly higher in comparison to the ALG COL films. Followed by, Pereira [39] has illustrated the thickness of ALG/*Aloe vera* film between  $59.7$  and  $75.3\ \mu\text{m}$ . Wang [40] in their work depicted that the thickness of the ALG/COL film was nearest to  $0.01\text{ mm}$ . Hence in the present case, the increase in film thickness was observed due to the incorporation of different proportions of COL and GLY.

#### 3.4.2. Film transparency and light transmission property

An increase in the COL content increased the transparency of the films, the developed films exhibited higher transparency, which is of great importance for the proposed application. The light transmission and transparency property has been computed and represented in Figure 4. The films were placed on glass slides with a white background for comparison of visualization and transparency (Figure 5). The results showed that the SA film alone exhibited the least transparency as  $0.038 \pm 0.004\%$  and the SACG 90/10 showed maximum transparency of  $1.015 \pm 0.01\%$ . The light transmittance and transparency are key characteristics of materials with wound healing properties [41]. Moreover, the higher intensity of visible light transmission is crucial for various skin based

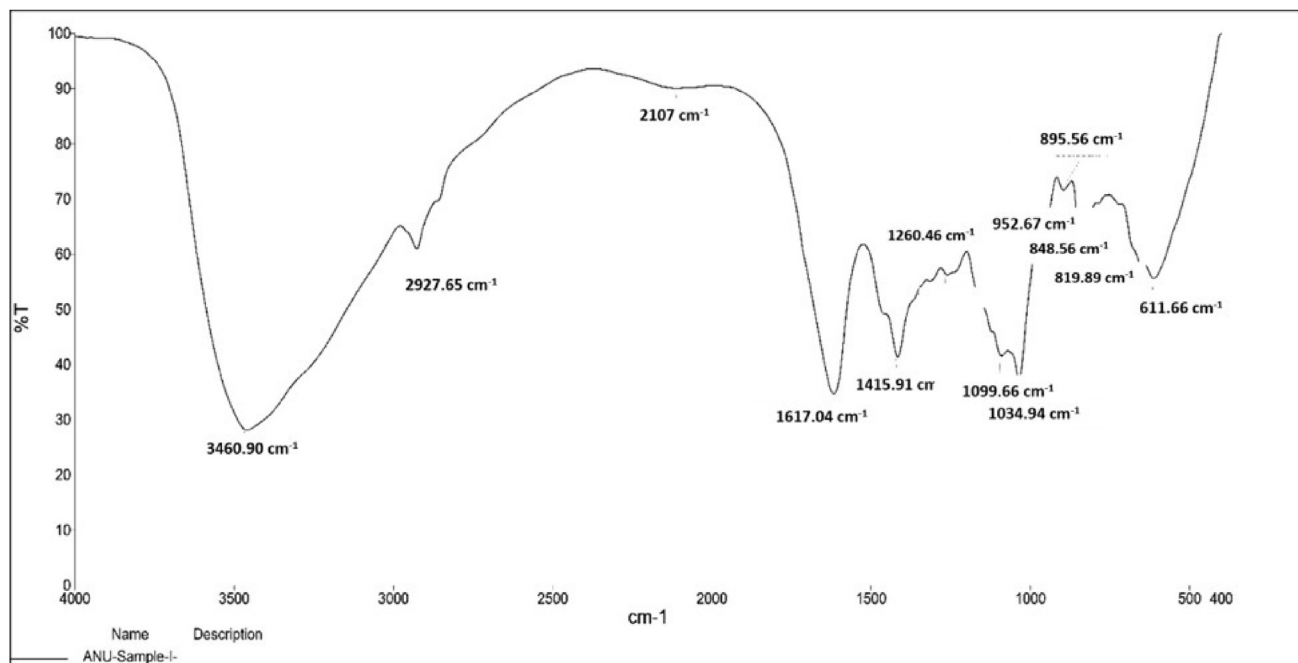


Figure 1. FT-IR spectrum of SA extracted from brown seaweed, *T. conoides*.

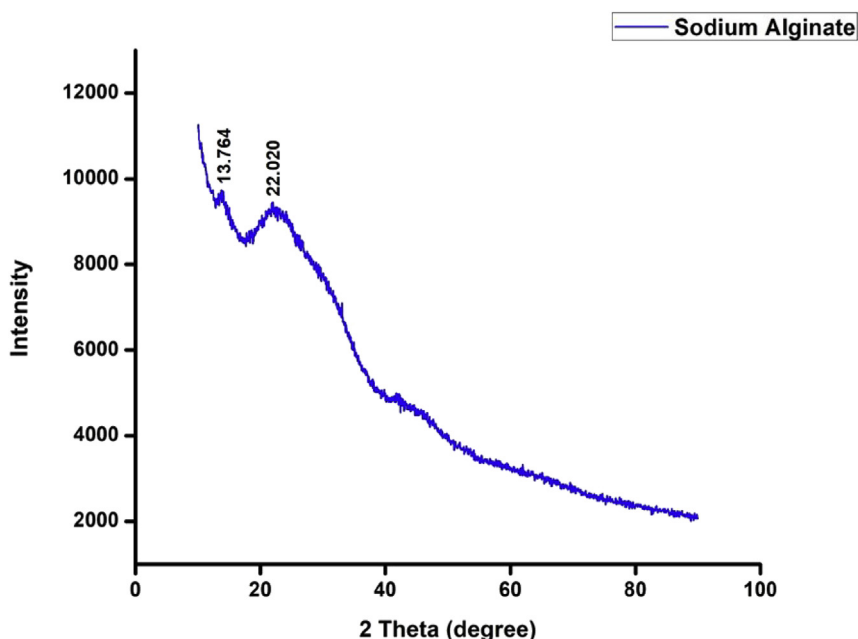


Figure 2. XRD Spectrum of purified SA from *T. conoides*.



Figure 3. SA films casted in different molds such as aluminum foil. (A); Petri plate of 5 cm diameter. (B); Petri plate of 12 cm diameter. (C) and recovery of the film from 12 cm dish (D).

Table 1. The thickness of the SA and SA/COL films with and without GLY.

Sr. No.	Formulation code	Thickness (µm)
1.	SA	50.1 ± 1.8
2.	SAG	52 ± 1.5
3.	SACG60/40	58.2 ± 1.6
4.	SAC60/40	54.6 ± 1.5
5.	SACG90/10	64.6 ± 1.5
6.	SAC90/10	61.8 ± 1.7

Values represent the mean of triplicates.

applications as it avails the healing of the wound and its observation without removal of the hydrogel [20].

### 3.4.3. Swelling behavior

The swelling behavior of the ALG based microfilms was found to vary based on the proportion of COL (Table 2). Since the GLY percentage was maintained constant the role of COL along with SA in swelling of the films was highly significant. The higher ratio of COL showed a lower

swelling index compared to the 60/40 ratio in the presence or absence of GLY. The SA combined with GLY and COL (60/40) film showed the highest swelling index of  $189.68 \pm 1.38\%$  whereas the lowest swelling index was possessed by SA GLY film. Saari [42] reported the swelling ratio of the SA/gelatin (G) film in the range of 72.52% (SA/G 70/30) and 90.1% for SA/G 30/70. According to them, the high swelling ability of the hydrogels was attributed to the hydrophilic functional groups such as  $\text{NH}_2^-$  and  $\text{COO}^-$  from the biopolymers. Good swelling hydrogels are key features of a good wound dressing agent. Hence, both SACG 60/40 and SAGC 90/10 could be developed as potent wound dressing material. As the developed hydrogel has wound dressing potential, its capacity to absorb aqueous solutions is fundamental. This feature also determines the ability of these films to absorb any exudate from the wound, avoids maceration and maintains a moist environment for faster wound healing.

### 3.4.4. Protein degradation activity of film

The anti-inflammatory activity of Standard drug (Diclofenac Sodium) was found to be  $73 \pm 1.70\%$ . The SACG90/10 film showed the highest anti-inflammatory activity of  $81.3 \pm 1.77\%$ , whereas, minimum activity was possessed by SA film as  $62.19 \pm 1.21\%$  (Figure 6). The standard and the sample concentrations were standardized as 50 µg/ml. By date, no

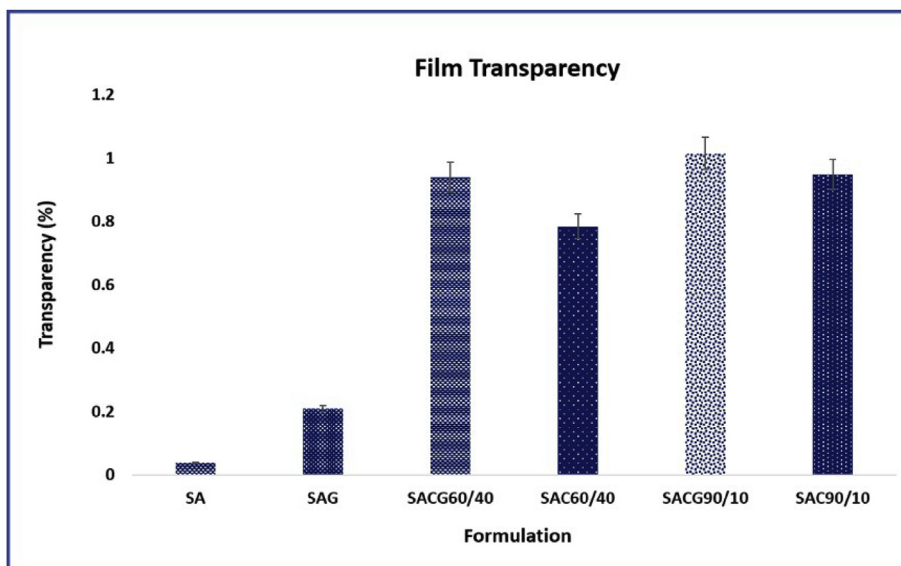


Figure 4. Comparative analysis of transparency among the formulated ALG based films.

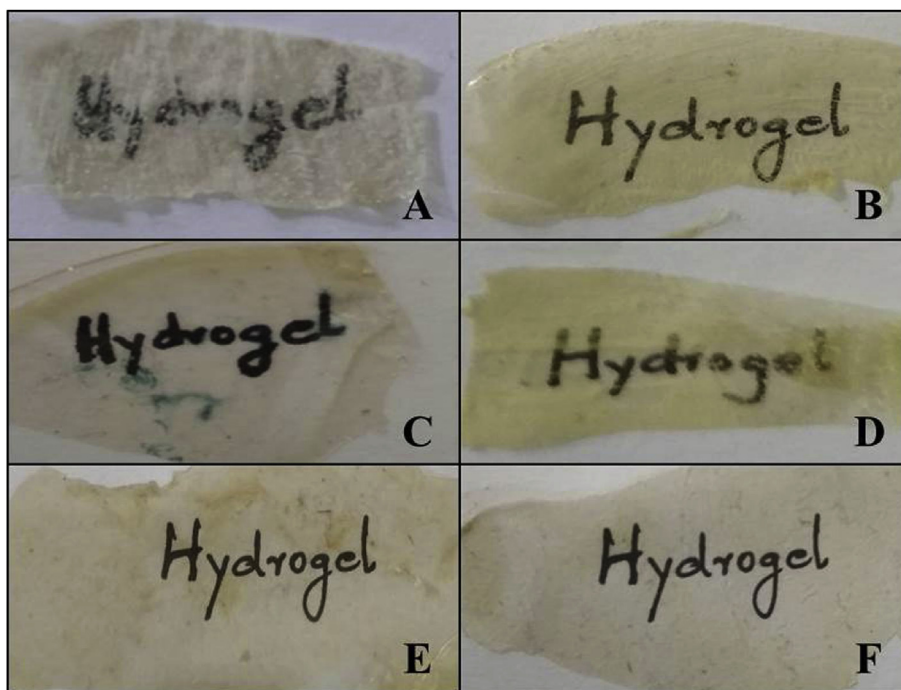


Figure 5. ALG based films for wound healing indicating transparency and thickness. (A) Sodium alginate film – SA. (B) Sodium alginate film with glycerol – SAG. (C) Sodium alginate and collagen in the ratio 60:40 with glycerol – SACG60/40. (D) Sodium alginate and collagen in the ratio 60:40 without glycerol – SAC60/40 (E) Sodium alginate and collagen in the ratio 90:10 with glycerol – SACG90/10. (F) Sodium alginate and collagen in the ration 90:10 without glycerol – SAC90/10.

Table 2. Swelling Index of formulated ALG based films.

Sr. No.	Formulation code	Swelling Index (%)
1.	SA	102.91 ± 1.72
2.	SAG	89.29 ± 0.53
3.	SACG60/40	189.68 ± 1.38
4.	SAC60/40	168.59 ± 0.69
5.	SACG90/10	174.57 ± 1.01
6.	SAC90/10	162.69 ± 1.03

Values represent the mean of triplicates.

such significant anti-inflammatory response has been reported from commercially available alginate hydrogel that was subcutaneously injected into mice [43]. Further, there is no recorded anti-inflammatory activity of the extracted ALG. Hence, the above evaluation has no other results to be compared with.

### 3.5. ALG microbeads encapsulated with an anticancer drug, tamoxifen

#### 3.5.1. Bead dimensions

All the ALG beads of varying combinations of drugs and ALG were prepared as uniform beads using a 22G syringe under magnetic stirring (Figure 7). The beads possessed a diameter of  $1 \pm 0.05$  mm and a

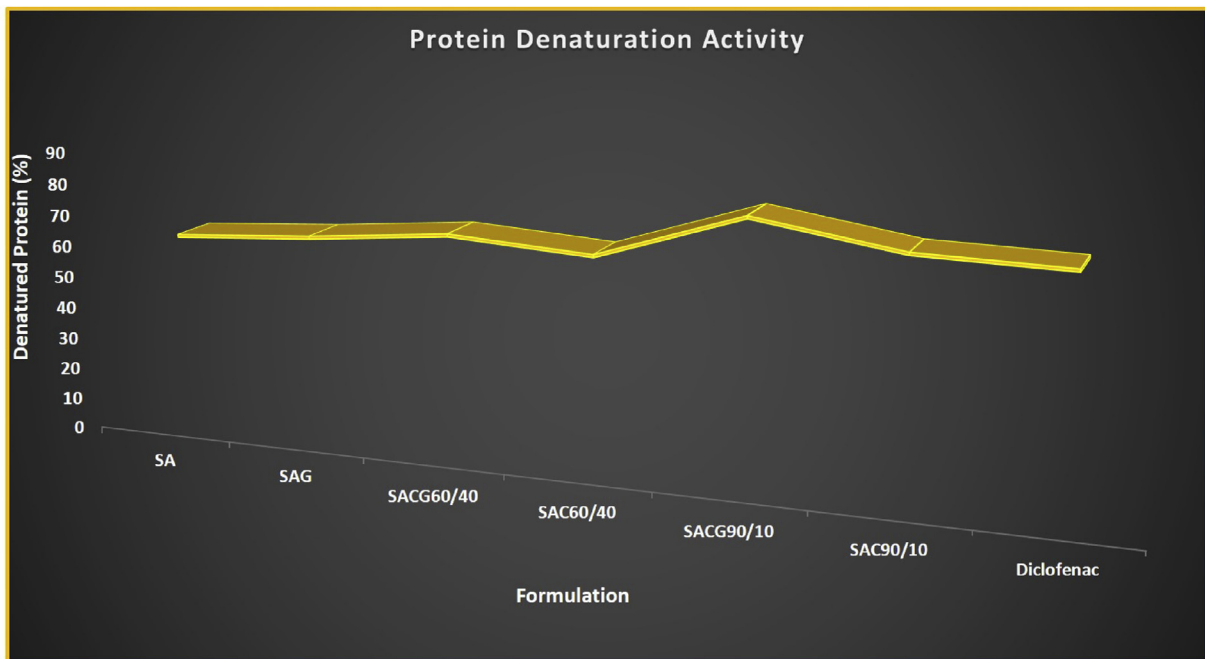


Figure 6. Protein Denaturation activity of ALG based beads.

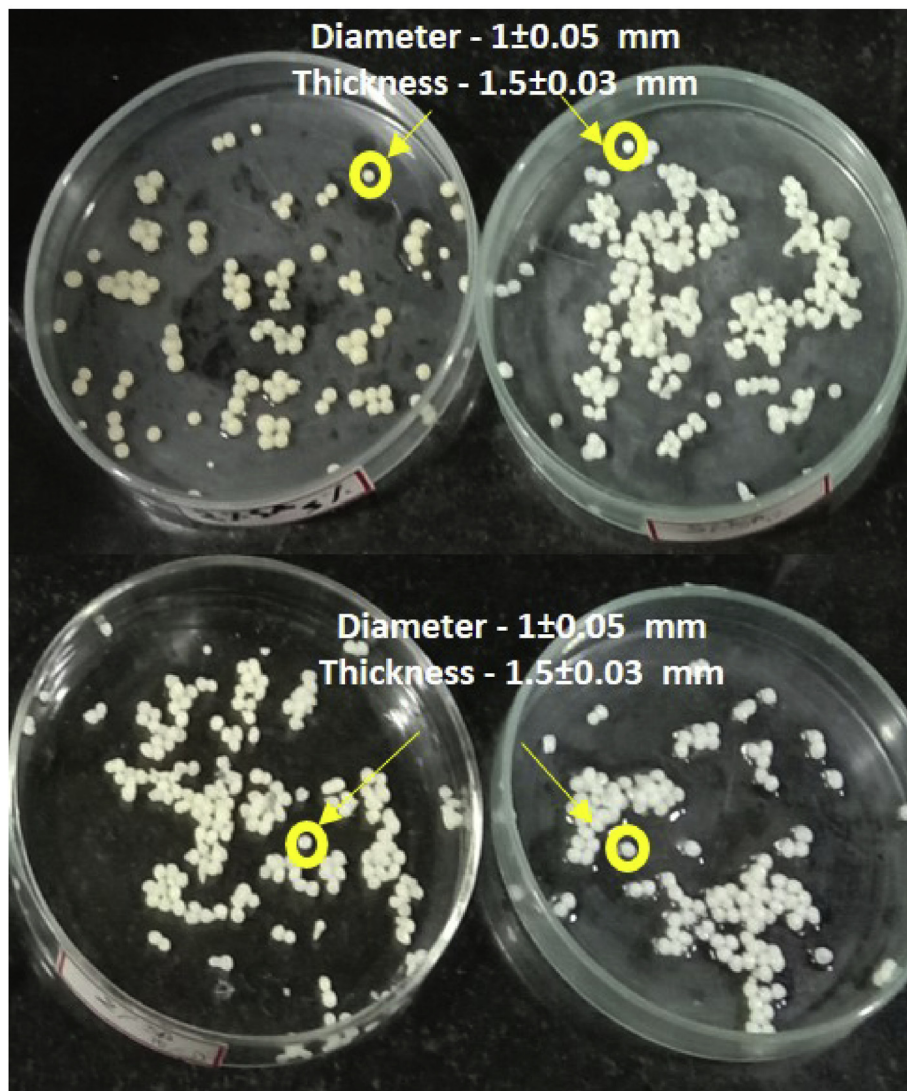


Figure 7. SA beads encapsulated with the standard anticancer drug, Tamoxifen.

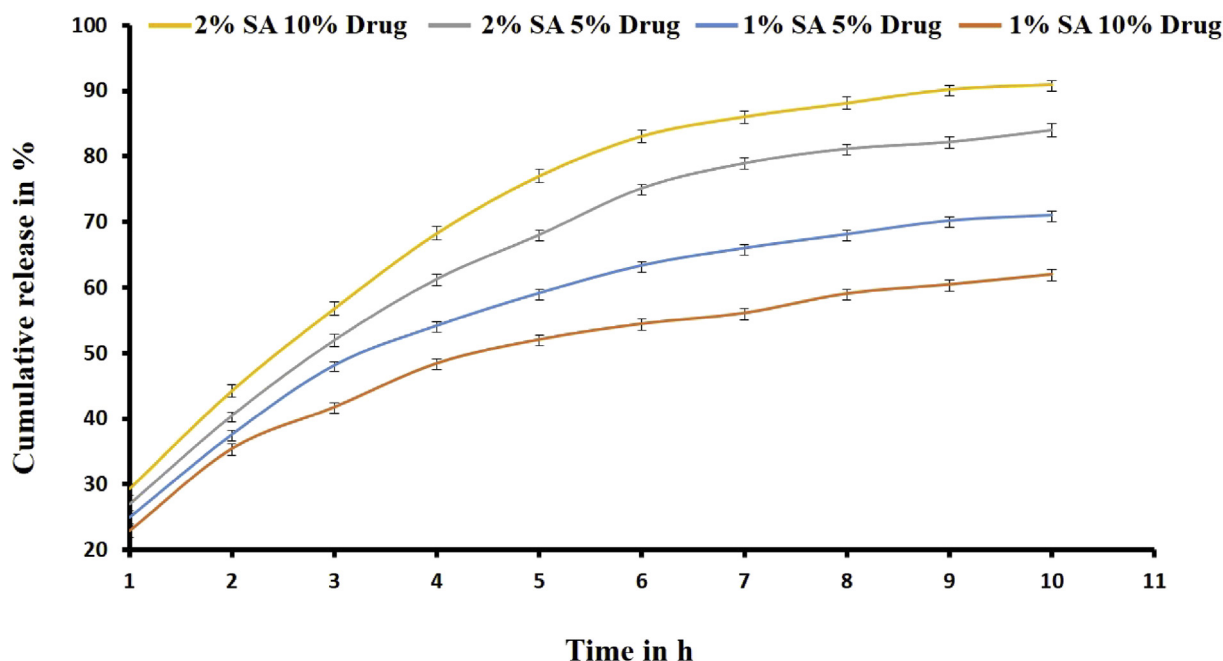


Figure 8. Schematic representation Drug release from ALG beads.

thickness of  $1.5 \pm 0.03$  mm in their wet state. Olukman [44] reported the size of ALG beads encapsulated with 5-Fluorouracil as 0.55–1.25 mm in diameter. In addition, the average size of celecoxib loaded beads (ALG and ALG/chitosan) between 715 and 896  $\mu\text{m}$  was documented by Seagle [45].

### 3.5.2. Swelling index of ALG beads

The ALG beads indicated a significant variance in the swelling ratio amongst each other. The 1% SA and 5% Drug exhibited a swelling ratio of  $101 \pm 1.63\%$ , whereas the same percentage of ALG loaded with 10% drug was swollen up to  $240 \pm 1.3\%$ . The 2% SA with 5% and 10% drug exhibited a swelling ratio of  $120 \pm 1.25\%$  and  $180 \pm 1.29\%$  respectively. In the studies of Bajpai and Kirar [46], where CA/poly (SA) beads were formed using calcium ALG/poly (sodium acrylate), swelling behavior of the beads was observed. The beads exhibited a maximum swelling value of 273% in 1 h and the swelling ratio decreased gradually up to 174% that extended over a total duration of 18 h. Therefore, it is a notable observation that SA hydrogel obtained from natural sources had a higher swelling index in comparison with the commercially purchased SA as reported in their paper.

### 3.5.3. Drug entrapment efficiency

The DEE of the drug increased with the increase in ALG concentration, however, calcium chloride cross-linker was fixed at a concentration of 5%. This effect is due to the increase in the viscosity of the polymer solution that in turn increased the droplet size during the addition of the polymer solution to the cross-linking solution. The DEE of the beads was found to be a maximum in 2% SA 10% Drug ( $91 \pm 1.27\%$ ) and minimum in 1% SA 10% Drug ( $63 \pm 1.01\%$ ). The 1% SA 5% Drug showed entrapment efficiency of  $71 \pm 1.59\%$  and 2% SA 5% Drug had an efficiency of  $84 \pm 0.90\%$ . DEE is a major property of a carrier molecule to understand its sustained release kinetics. The maximum encapsulation efficiency was found to be 79.75% and 93.07% for SA and SA/CMC blend respectively for the formulations in the work of Lee [47]. In addition, in the release studies of ALG microspheres encapsulated with tetanus toxoid, the encapsulation efficiency reached almost 50% and the burst effect was relatively low in their ALG microspheres [48]. Therefore, the extracted ALG from *T. conoides* remains significant in the DEE when compared to other commercial ALG beads.

### 3.5.4. Drug release study for tamoxifen encapsulated ALG beads

The *in vitro* drug release studies for the beads in the HCl medium (pH 1.2) were carried out initially for 2 h and later in phosphate buffer (pH 7.4) for 10 h. The ALG based beads released negligible amounts (<3%) of the drug in the HCl, due to the poor dissolution of ALG in an acidic pH (<3). However, the presence of a trace amount of drugs as turbidity could be due to the surface-adhered drug. The ALG bead prolonged around  $62 \pm 0.70\%$  -  $91 \pm 0.56\%$  of the drug release after 10 h of study in Phosphate Buffer (Figure 8). The drug release profiles of the formulated beads were 1% SA 5% Drug ( $71 \pm 0.57\%$ ), 1% SA 10% Drug ( $62 \pm 0.70\%$ ), 2% SA 5% Drug ( $84 \pm 0.95\%$ ) and 2% SA 10% Drug ( $91 \pm 0.56\%$ ). Due to the hydrophilic nature of ALG, the release of encapsulated drug payloads could follow different mechanisms. The poorly water-soluble drugs are released only through the matrix erosion method unlike the water-soluble drugs [49]. Likewise, the release of small drug molecules was more through the swollen ALG pores of 5 nm size [50]. Thus, the extended period of drug release in the present study attributes to the development of the ALG hydrogel as a sustained drug delivery agent.

## 4. Conclusion

SA or sodium salt of alginate was synthesized from *T. conoides*. The primary objective of this study was to formulate a hydrogel with targeted biomedical applications. Herewith, two hydrogel formulations of ALG were synthesized such as ALG/COL microfilm for wound healing and ALG microbead with an anticancer drug, Tamoxifen for sustained drug release. The ALG/COL/GLY wound healing film with a SA to COL nm ratio of 60/40 and 90/10 presented notable anti-inflammatory activity, swelling index and transparency that are essential characteristics for a wound-healing agent for exudate absorption and faster wound healing. Likewise, the 2% SA hydrogel with both 5% and 10% drug revealed good swelling index, DEE and drug release profile for development as a sustained drug release hydrogel carrier. The formed ALG microbead has prospective applications in the drug delivery system for sustained-release of the water-insoluble drugs like Tamoxifen. Further, the novel formulation of ALG from brown seaweed and COL from stingray fish may be applied in the development of cost-effective microfilm with potential wound healing properties. Hence through the present study, the hydrogel

capability of ALG from *T. conoides* has been proved for biomedical applications and in pharmacology.

## Declarations

### Author contribution statement

Naidu Kavitha: Conceived and designed the experiments; Performed the experiments; Wrote the paper.

Thennarasu P. Karunya: Performed the experiments.

Shankar Kanchana: Performed the experiments; Wrote the paper.

Kumar Mohan: Analyzed and interpreted the data.

Ramachandiran Sivaramakrishnan & Selvaraj Uthra: Performed the experiments.

Kalimuthu Kapilan: Contributed reagents, materials, analysis tools or data.

Dinakarkumar Yuvaraj: Performed the experiments; Analyzed and interpreted the data.

Muthuvel Arumugam: Contributed reagents, materials, analysis tools or data.

### Funding statement

This work was supported by the Department of Science and Technology (DST) sponsored National Facility for Marine Natural Products and Drug Discovery Research' [G4(2)/21343/2017] and Ministry of Earth Sciences (MoES) sponsored Programme 'Drugs from the Sea' [G4(2)/14748/2016].

### Competing interest statement

The authors declare no conflict of interest.

### Additional information

No additional information is available for this paper.

## References

- 1] M.J. Costello, C. Chaudhary, Marine biodiversity, biogeography, deep-sea gradient and Conversion, *Curr. Biol.* 5 (2017) R511–R527, 693.
- 2] S. Shukla, M. Kim, Marine natural flora: a potent source of anticancer metabolite, *Indian J. Geomar. Sci.* 45 (2016) 1412–1421.
- 3] A.H. Buschmann, C. Camus, J. Infante, A. Neori, Á. Israel, M.C. Hernandez Gonzalez, S.V. Pereda, J. Luis, G. Pinchetti, A. Golberg, N. Tadmor-Shalev, A.T. Critchley, Seaweed production: overview of the global state of exploitation, farming and emerging research activity, *Eur. J. Phycol.* 52 (2017) 391–406.
- 4] K. Alba, V. Kontogiorgos, Seaweed Polysaccharides (Agar, Alginate Carrageenan), University of Huddersfield, Elsevier Journal, Huddersfield, United Kingdom, 2003.
- 5] L.E. Rioux, S.L. Turgeon, M. Beaulieu, Characterization of polysaccharides extracted from brown seaweed, *Carbohydr. Polym.* 69 (2007) 530–537.
- 6] A. Ali, S. Ahmed, Recent advances in edible polymer based hydrogels as a sustainable alternative to conventional polymers, *J. Agric. Food Chem.* (2018).
- 7] K.Y. Lee, D.J. Mooney, Alginate properties and biomedical applications, *Prog. Polym. Sci.* 37 (2010) 106–126.
- 8] E.M. Ahmed, Hydrogel: preparation, characterization and application, *J. Adv. Sci.* (2013). Elsevier.
- 9] K.S. Soon, S.L. Hii, C.L. Wong, L.K. Leong, K.K. Woo, Physicochemical Properties of marine COL-ALG Biomaterial, 2017, p. 1901.
- 10] H. Xie, X. Chen, X. Shen, Y. He, W. Chen, Q. Luo, K. Li, Preparation of chitosan-collagen-alginate composite dressing and its promoting effects on wound healing, *Int. J. Biol. Macromol.* 107 (2018) 93–104.
- 11] M. Criado-Gonzalez, M. Fernandez-Gutierrez, J. San Roman, C. Mijangos, R. Hernandez, Local and controlled release of tamoxifen from multi (Layer-By-Layer) alginate/chitosan complex systems, *Carbohydr. Polym.* (2018).
- 12] A. Kaczmarek-Pawelska, Alginate-Based Hydrogels in Regenerative Medicine, in: *Book: Alginate*, IntechOpen, 2019, pp. 1–16.
- 13] G.Z. Jin, H.W. Kim, Efficacy of collagen and alginate hydrogels for the prevention of rat chondrocyte dedifferentiation, *J. Tissue Eng.* 9 (2018).
- 14] G. Montalbano, S. Toumpaniari, A. Popov, P. Duan, J. Chen, K. Dalgarno, A.M. Ferreira, Synthesis of bioinspired collagen/alginate/fibrin based hydrogels for soft tissue engineering, *Mater. Sci. Eng. C* 91 (2018) 236–246.
- 15] T.A. Fenoradosoa, G. Ali, C. Delattre, Extraction and characterization of an alginate from the brown seaweed *Sargassum turbinarioides* Grunow, *J. Appl. Phycol.* 22 (2010) 131–137.
- 16] O.H. Lowry, N.J. Rosebrough, A.L. Farr, R.J. Randall, Protein measurement with the Folin phenol reagent, *J. Biol. Chem.* 193 (1951) 265–275.
- 17] M. DuBois, K.A. Gilles, J.K. Hamilton, P.A. Rebers, F. Smith, Colorimetric method for determination of sugars and related substances, *Anal. Chem.* 28 (1956) 350–356.
- 18] T. Bitter, H.M. Muir, A modified uranic acid carbazole reaction, *Anal. Biochem.* 4 (1962) 330–334.
- 19] P. Archana, T. Samatha, B. Mahitha, N.R. Chamundeswari, Preliminary phytochemical screening from leaf and seed extracts of *Senna alata* L. Roxb- an ethno medicinal plant, *Int. J. Pharm. Biol. Res.* 3 (2012) 82–89.
- 20] R. Pereira, A. Carvalho, D.C. Vaz, M.H. Gill, A. Mendes, P. Bartolo, Development of novel alginate based hydrogel films for wounding healing application, *Int. J. Boil. Macromole.* 52 (2013) 221–230.
- 21] K. Norajit, K.M. Kim, G.H. Ryu, Comparative studies on the characterization and antioxidant properties of biodegradable alginate films containing ginseng extract, *J. Food Eng.* 98 (2010) 377–384.
- 22] K. Gunathilake, K. Ranaweera, H. Rupasinghe, *In vitro* anti-inflammatory properties of selected green leafy vegetables, *Biomed* 6 (2018) 107.
- 23] S. Mandal, S.S. Kumar, B. Krishnamoorthy, S.K. Basu, Development and evaluation of calcium alginate beads prepared by sequential and simultaneous method, *Brazilian J. Pharm. Sci.* 46 (2010) 785–793.
- 24] R. Kusumawati, J. Basmal, B.S.B. Utomo, Characteristics of SA extracted from *Turbinaria* sp. and *sargassum* sp, *Squalen Bull. Mar. Fish. Postharvest Biotechnol.* 13 (2018).
- 25] S. Jothisaraswathi, B. Babu, R. Rengasamy, Seasonal studies on alginate and its composition II: *Turbinaria conoides* (J.Ag.) Kütz. (Fucales, Phaeophyceae), *J. Appl. Phycol.* 18 (2006) 161–166.
- 26] R.H. McDowell, Properties of Alginates, fourth ed., Alginate industries. Ltd., London, 1977, p. 67.
- 27] M. Nasir, M.S. Butt, F.M. Anjum, K.A. Sharif, R. Minhas, Effect of moisture on the shelf life of wheat flour, *Int. J. Agric. Biol.* 5 (2003) 458–459.
- 28] T.S. Parreidt, K. Müller, M. Schmid, Alginate-based Edible Films and Coatings for Food Packaging Applications, *Foods* 7 (2018) E170.
- 29] G. Kokilam, S. Vasuki, N. Sajitha, Biochemical composition, alginic acid yield and antioxidant activity of brown seaweeds from Mandapam region, Gulf of Mannar. *J. Applied Pharm. Sci.* 3 (2013) 099–104.
- 30] B. Larsen, D.M.S.A. Salem, M.A.E. Sallam, M.M. Mishrikey, A.I. Beltagy, Characterization of the alginates from algae harvested at the Egyptian Red Sea coast, *Carbohydr. Res.* 338 (2003) 2325–2336.
- 31] B. Larsen, O. Smidsrød, T. Painter, A. Haug, Development of compositional heterogeneity in alginate degraded in homogeneous solution, *Acta Chem. Scand.* 24 (1970) 726–728.
- 32] G.K. Kumar, G. Battu, K.N.S. Raju, Isolation and evaluation of tamarind seed polysaccharide being used as a polymer in pharmaceutical dosage forms, *Res. J. Pharm. Biol. Chem. Sci.* 2 (2011) 274–290.
- 33] L. Zu, Y. Zhao, G. Gu, Recent development in the synthesis of natural saponins and their derivatives, *J. Carbohydr. Chem.* 33 (2014) 269–297.
- 34] P. Li, Y.N. Dai, J.P. Zhang, A.Q. Wang, Q. Wei, Chitosan-alginate nanoparticles as a novel drug delivery system for nifedipine, *Int. J. Biomed. Sci.* 4 (2008) 221–228.
- 35] V. Garcia-Ríos, E. Ríos-Leal, D. Robledo, Y. Freile-Pelegrin, Polysaccharides composition from tropical brown seaweeds, *Phycol. Res.* 60 (2012).
- 36] D. Fang, Y. Liu, S. Jiang, J. Nie, G. Ma, Effect of intermolecular interaction on electrospinning of sodium alginate, *Carbohydr. Polym.* 85 (2011) 276–279.
- 37] H. Helmiyati, M. Aprilliza, Characterization and properties of SA from brown algae used as an eco-friendly superabsorbent, *IOP Conf. Ser. Mater. Sci. Eng.* 188 (2017), 012019.
- 38] P. Sundarajan, P. Eswaran, A. Marimuthu, S.B. Lakshmi, P. Kannaiyan, One pot synthesis and characterization of alginate stabilized semiconductor nanoparticles, *Bull. Korean Chem. Soc.* 33 (2012) 3218–3224.
- 39] R. Pereira, A. Mendes, P. Bartolo, Alginate/Aloe vera hydrogel films for biomedical application, *CIRP* 5 (2013) 210–215.
- 40] Z. Wang, S. Hu, H. Wang, Scale-up preparation and characterization of COL/SA blend films, *J. Food Qual.* 10 (2017).
- 41] J.S. Boateng, K.H. Matthews, H.N. Stevens, G.M. Eccleston, Wound healing dressings and drug delivery systems: a review, *J. Pharm. Sci.* 97 (2008) 2892–2923.
- 42] A. Saarai, T. Sedlacek, V. Kasparkova, T. Kitano, P. Saha, On the characterization of sodium alginate/gelatin-based hydrogels for wound dressing, *J. Appl. Polym. Sci.* 126 (2012) E79–E88.
- 43] J. Lee, K.Y. Lee, Local and sustained vascular endothelial growth factor delivery for angiogenesis using an injectable system, *Pharm. Res.* 26 (2009) 1739–1744.
- 44] M. Olukman, O. Sanli, E. Kondolot Solak, Release of anticancer drug 5-fluorouracil from different ionically crosslinked alginate beads, *J. Biomaterials Nanobiotechnol.* 3 (2012) 469–479.
- 45] L. Segale, L. Giovannelli, P. Mannina, F. Pattarino, Calcium alginate and calcium alginate-chitosan beads containing celecoxib solubilized in a self-emulsifying phase, *Sci. Tech. Rep. (Cairo)* (2016) 5062706.
- 46] S.K. Bajpai, N. Kirar, Swelling and drug release behaviour of calcium alginate/poly (sodium acrylate) hydrogel beads, *J. Des. Monomers Polym.* 19 (2016) 88–98.
- 47] C.H. Lee, P.N. Lakshmi, P. Srinivasa, Optimization studies for encapsulation and controlled release of curcumin drug using Zn+2 cross-linked ALG and carboxy methylcellulose blend, *J. Polym. Res.* 26 (2019).

- [48] M. Tafaghodi, S.A. Sajadi Tabasi, M.R.J. Jaafari, Formulation, characterization and release studies of alginate microspheres encapsulated with tetanus toxoic, *Biomater. Sci. Polym. Ed.* 17 (2016) 909–924.
- [49] A. Sosnik, Alginate particles as platform for drug delivery by the oral route: state of the Art, *ISRN pharm* (2014).
- [50] M. Otterlei, K. Ostgaard, G. Skjak-Braek, O. Smidsrod, P. Soon-Shiong, T. Espevik, Induction of cytokine production from human monocytes stimulated with alginate, *J. Immunother.* 10 (1991) 286–291.